

## A NEW LIBRARY OF STELLAR OPTICAL SPECTRA

DAVID R. SILVA<sup>1</sup>

University of Michigan; and Kitt Peak National Observatory, National Optical Astronomical Observatories<sup>2</sup>

AND

MARK E. CORNELL

McDonald Observatory, University of Texas, RLM 15.308, Austin, TX 78712

*Received 1991 August 12; accepted 1992 January 10*

### ABSTRACT

A new digital optical stellar library is presented. It consists of spectra covering 3510–8930 Å at 11 Å resolution for 72 different stellar types. These types extend over the spectral classes O–M and luminosity classes I–V. Most spectra are of solar metallicity stars but some metal-rich and metal-poor spectra are included. This new library is quantitatively compared to two previously published libraries. The library has been submitted to the Astronomical Data Center at the NASA Goddard Space Flight Center for convenient distribution. It is also available via anonymous ftp over Internet.

*Subject headings:* atlases — techniques: spectroscopic

### 1. INTRODUCTION

Digital optical stellar libraries are important for three general areas of astrophysical problems: stellar classification, stellar population synthesis, and theoretical stellar atmosphere verification. In the first application, stellar libraries are particularly important in the growing use of automatic spectral classification of large digital data bases (Kurtz 1984). Second, empirical population synthesis uses stellar libraries as sets of basis vectors for decomposing composite spectra (e.g., Silva 1991) while evolutionary population synthesis uses stellar libraries to model composite spectra as a function of time and star formation history (e.g., Guiderdoni & Rocca-Volmerange 1987). Last, digital stellar libraries are useful for the testing of the increasingly sophisticated theoretical stellar atmosphere models now becoming available (e.g., Kurucz 1991).

There are several general technical and astrophysical criteria for good stellar libraries. Technical criteria include photometric precision, spectral coverage, and spectral resolution. Although specific design goals are situation dependent, ideal optical libraries would have signal-to-noise ratios in excess of 100, spectral baselines spanning as much of the interval 3200–10,000 Å as possible, and spectral resolutions between 0.1 and 10 Å FWHM. Furthermore, consistent and accurate photometric calibration is essential. The primary astrophysical criterion is to cover temperature, metallicity, and surface gravity (TZG) parameter space as thoroughly as possible. Note that since stellar luminosity is determined by a combination of temperature, metallicity, and surface gravity, it is an imperfect indicator of surface gravity alone.

All currently available libraries violate one or more of these criteria. Older published optical spectrophotometric libraries

(Spinrad & Taylor 1971; O'Connell 1973; Breger 1976; Joly 1974; Pritchett & van den Bergh 1977; MacFarlane 1979; Gunn & Stryker 1983) suffer from low spectral resolution (20 Å or worse) precluding their use in many modern situations. While the Jacoby, Hunter, & Christian (1984; hereafter JHCLIB) and Pickles (1985; hereafter PICKLIB) libraries have better resolution, neither are ideal. JHCLIB has good spectral resolution (3–4 Å), good spectrophotometric calibration, and good temperature-luminosity coverage of the H-R diagram. However, it suffers from three shortcomings. First, it only spans 3510–7240 Å, missing such important near-IR lines as the TiO bands between 7500 Å and 1.1 μm, Na I λ8190, Ca II λλ8498, 8542, 8662, the Wing-Ford band at 9910 Å, and He I λ10830. Second, while dwarf-supergiant separation is adequate, there exists some dwarf-giant classification confusion, particularly among hotter stars (G. H. Jacoby 1991, private communication). Third, the vast majority of the stars in JHCLIB have approximately solar metallicities, making JHCLIB a poor match for both old, metal-rich populations (i.e., the nuclei of early type galaxies) and old, metal-poor populations (i.e., globular clusters). In contrast, PICKLIB has both extended spectral coverage (out to 1 μm) and extended metallicity coverage for giant stars. Unfortunately, sections of the PICKLIB spectra consist of very low (50 Å) resolution data, usually beyond 7000 Å. Furthermore, the bluest PICKLIB spectra have questionable photometric calibration blueward of 4000 Å (see discussion below).

An effort to improve upon the current situation is reported here. Newly acquired and previously published data have been combined to form a new digital optical library primarily intended for use in empirical population synthesis (see Silva 1991). The resultant library spans 3510–8930 Å at an effective resolution of 11 Å FWHM with good temperature and luminosity coverage but poor metallicity coverage. Nevertheless, it offers significant advantages over many previously published libraries.

<sup>1</sup> Present Address: NOAO/KPNO, P.O. Box 26732, Tucson, AZ 85726-6732.

<sup>2</sup> NOAO is operated by the Association of Universities for Research in Astronomy, Inc., under contract with the National Science Foundation.

## 2. DATA ACQUISITION AND REDUCTION

### 2.1. Original Sources of Individual Stars

An effort was made to observe mainly stars with TZG parameters derived from stellar atmosphere models of high dispersion data. Such models provide a more accurate characterization of the TZG parameters of an individual star than its published MK stellar classification. The initial sample was selected from Cayrel de Strobel et al. (1985), a catalog of stars with precise stellar atmosphere studies published before 1983. Additional stars came from Faber et al. (1985) (metal-rich G and K giant stars), Luck & Bond (1985) (metal-poor G giant stars), and Laird, Carney, & Latham (1988) (metal-poor and metal-rich F, G, and K dwarf stars). Additional M stars without detailed atmosphere models were selected from Keenan (1983) and Turnshek et al. (1985). These M stars were assumed to be solar metallicity. Many of the solar metallicity stars in Jacoby et al. (1984) were also reobserved as a consistency check.

### 2.2. New Observations

Stellar data for a large number of individual stars were acquired during seven observing runs between 1988 December and 1989 May. The individual runs are listed in Table 1; their general characteristics are described below.

#### 2.2.1. MDM Data

Data in the spectral regime 4500–9250 Å were obtained at the Michigan-Dartmouth-MIT (MDM) Hiltner 2.4 m telescope using the Mark III grism spectrograph. Two 300 l mm<sup>-1</sup> grisms were used: grism No. 4 (G4) blazed at  $\approx$ 5000 Å, covering 4360–7100 Å, and grism No. 2 (G2) blazed at  $\approx$ 8200 Å, covering 6750–9250 Å. An order blocking filter was necessary when using G2. All observations were made through a 1''.2 slit resulting in a spectral resolution of  $\approx$ 11 Å FWHM. Either a Thomson-CSF TH7861 four-phase CCD or a Texas Instruments TI4849 virtual phase CCD (Luppino 1989) was used. A relatively narrow slit was used to increase spectral resolution. Such a narrow slit creates the danger of wavelength-dependent light loss due to differential atmospheric refraction. To minimize such losses, the slit was always rotated to the appropriate position angle as tabulated by Filippenko (1982). Since the Mark III spectrograph operates in a long-slit configuration, it

was possible to increase photometric precision and avoid CCD saturation by cyclically trailing each star along the slit throughout the exposure.

Observations of photometric calibration stars were made during each run. Standard stars were selected from either the “IRS Standard Star Manual” (Barnes & Hayes 1982) or “The IIDS Standard Star Manual” (Strom 1979). Typically, four to six such observations were made per night. An effort was made to observe either HD 19445 or HD 84937 every night to allow night-to-night and run-to-run calibration comparisons. Due to the combination of narrow slit, large effective point spread function, and variable sky conditions, absolute calibration was precluded. However, comparison of the repeated HD 19445 and HD 84937 observations shows that continuum shape was repeatable at the 1% level for all the MDM data used.

These KPNO flux standards have two intrinsic problems which affected this project. First, calibration data beyond 8750 Å is sparsely sampled and sometimes of lower resolution. Fortunately, the continua of the observed standard stars change smoothly in that spectral regime allowing acceptably accurate calibrations. Nevertheless, some continuum shape uncertainty is introduced. The second problem, the overall low resolution ( $\approx$ 50 Å) of these calibration data, creates difficulties when calibrating sharp continuum features in higher resolution data. While this does not affect the MDM bandpasses, it can be a problem near the 4000 Å break (see Jacoby et al. 1984). Furthermore, accurately interpolating over the absorption lines in the primary calibrators used here, HD 19445 and HD 84937, becomes more difficult at the higher resolution used here. All such problems could be alleviated in the future by using higher resolution data for stars with fewer absorption lines and more slowly varying continua in the optical window (see Massey et al. 1988 and Massey & Gronwall 1990).

The standard menagerie of arc lamps, bias frames, and flat field images were also obtained and used during data reduction as described below. During early runs, it was empirically determined that the Mark III exhibited only subpixel ( $\lesssim$ 1 Å) wavelength zero point shifts due to spectrograph flexure. For subsequent runs, arcs were only taken at the beginning and end of the night. Both twilight flats and incandescent flats created by “observing” an internal spectrograph flat lamp were obtained. The configuration of dome flat screen and illumination lamps at the Hiltner 2.4 m during this period yielded unacceptable dome flats; these flats were discarded.

TABLE 1  
OBSERVATION LOG

ID	Date	Telescope	Spectrograph	Grism	Detector
A .....	1988 Jan	MDM 2.4 m	MkIII	G4	TH7861
C .....	1988 Feb	MDM 2.4 m	MkIII	G4	TH7861
D .....	1988 Mar	SOKP 2.3 m	B&C	...	TI 800 × 800
E .....	1988 May	SOKP 2.3 m	B&C	...	TI 800 × 800
F.....	1989 Nov	MDM 2.4 m	MkIII	G2	TH7861
G.....	1989 Nov	MDM 2.4 m	MkIII	G4	TH7861
H.....	1989 Feb	MDM 2.4 m	MkIII	G4	TH7861
I.....	1989 Feb	MDM 2.4 m	MkIII	G2	TH7861
J.....	1989 May	MDM 2.4 m	MkIII	G4	TI 4849
K.....	1989 May	MDM 2.4 m	MkIII	G2	TI 4849

The IRAF<sup>3</sup> TWODSPEC package was used to perform preliminary data reductions. For reference, columns are aligned along the dispersion direction and rows along the spatial direction. Each night was independently reduced of all other nights as much as possible. A mean bias frame constructed from bias frames obtained at the beginning of the night was subtracted from all other frames. Bias-subtracted incandescent lamp frames were then median combined and normalized to produce a flat field frame. A illumination correction frame was constructed by dividing the flat field frame into a high signal-to-noise, bias subtracted twilight frame and then fitting low order polynomials to the average of  $\sim 80\text{--}100$  rows. The result was normalized and multiplied by the flat frame to produce the final spectral response frame. This frame was divided into all object frames. A wavelength rectification map was then constructed from measurements of arc lamp spectra while a spatial rectification map was constructed either from the spectra of untrailed stars displaced along the slit or from the spectrum of a flat lamp observed through a series of pinholes. These maps were constructed using Chebyshev polynomials with as low an order as possible to minimize high-frequency "ripples" in the solutions. Adequate wavelength rectification usually required a fifth order polynomial while spatial rectification only required a second or third order polynomial. During rectification, spectra were rebinned to  $5 \text{ \AA pixel}^{-1}$ .

After rectification, the trailed stellar spectra were extracted. As the stars observed were quite bright, sky subtraction was unnecessary. The extraction aperture was chosen to contain all columns  $3.0 \sigma$  above the "background," i.e., those columns outside of the trailed spectrum. The bright stars observed created some amount of scattered light which, for the brightest stars, made such a spectrum/background distinction difficult. While this is not a problem at the high end of the CCD response curve, at the low end this scattered light can make continuum determination uncertain at the 2%–5% level. Although attempts were made to correct for this effect, the ultimate solution was to discard the pixels most affected by this problem.

Extracted spectra were extinction corrected using the standard Kitt Peak extinction curve as tabulated within IRAF 2.8 and then flux calibrated using the standard star observations discussed above. Night-to-night and run-to-run comparison of flux standards indicated that the flux calibration was reliable and repeatable between  $4500\text{--}7000 \text{ \AA}$  and  $6900\text{--}9000 \text{ \AA}$  for G4 and G2, respectively. Individual observations were trimmed to these ranges.

### 2.2.2. SOKP Data

Blue data ( $3370\text{--}4700 \text{ \AA}$ ) were obtained at the Steward Observatory Kitt Peak (SOKP) Bok 2.3 m telescope using the B&C Spectrograph during two runs in the spring of 1988 (see Table 1). An UV enhanced Texas Instruments  $800 \times 800$  CCD was used. A  $1.5''$  slit and  $600 \text{ l mm}^{-1}$  grating blazed at  $\approx 3570 \text{ \AA}$  yielded an effective spectral resolution of  $\approx 3.8 \text{ \AA}$  FWHM. Standard star selection, slit rotation, and star trailing were all done in a manner analogous to the MDM observations. Due to operational restrictions, only dome flats were

obtainable during most nights of these runs. Fortunately, they proved sufficient.

Data reduction of the SOKP data followed the procedure outlined for the MDM data with the following two exceptions. First, as only dome flats were available for the most part, there was no separate response/illumination correction process. Second, the B&C spectrograph is known to have a significant amount of flexure which fortunately only appears significant in the wavelength zero point term. To account for this flexure, arc lamp frames were obtained after every stellar observation. During data reduction, the first arc frame of the night was fully mapped. Then, subsequent arc frames were cross-correlated against this frame to derive zero point offsets. Their associated stellar frames were then rectified using the original distortion maps with the appropriate zero point shift applied. Intercomparison of rectified arc lamp frames shows that this two-step process only introduces random dispersion errors. The SOKP stars were rebinned to  $1.88 \text{ \AA pixel}^{-1}$  and spanned  $3370\text{--}4700 \text{ \AA}$ .

### 2.3. Incorporation of Published Data

New data with complete spectral coverage were obtained for a limited subset of all the individual stars actually observed. Specifically, more stars were observed in the MDM red bandpasses than in the SOKP blue bandpass. Fortunately, many of the stars without new SOKP data were reobserved JHCLIB stars. Thus, blue data from JHCLIB has been extracted to provide complete wavelength coverage for all reobserved JHC stars with red MDM data but no blue SOKP data. The JHCLIB data was obtained from the Astronomical Data Center at the NASA Goddard Space Flight Center.

### 2.4. Astrophysical Parameters

A list of individual stars with complete spectral coverage is provided in Table 2. The list was sorted by metallicity (M), luminosity class (L), and effective temperature ( $T_e$ ), in that order. Table 2 includes the following

*Column (1).*—HD: the HD catalog number.

*Column (2).*—Other: the SAO catalog number if the prefix is "s" or Lowell Proper Motion Survey number (Giclas, Burnham, & Thomas 1972, 1978) if the prefix is "g."

*Column (3).*—Type: Spectral type from original reference. Stars from reference L and typed V\* are most likely to be dwarfs but may be some other luminosity class. See reference for details.

*Column (4).*—Observations: observing run codes from Table 1. Blue SOKP data: DE. MDM G4 data: ACGHJ. MDM G2 data: FIK. If not observed during runs D and E, blue data came from Jacoby et al. (1984) as described above.

*Column (5).*— $T_e$ : Assigned effective temperature. If reference code is L or FEH,  $T_e$  came from the original reference and is based on a stellar atmosphere analysis of the object. Otherwise, it was interpolated from tables in Schmidt-Kaler (1982) based on the assigned spectral type.

*Column (6).*—L: assigned luminosity class. If reference code is L, FEH, LB, or FFGB, then luminosity class based on stellar atmosphere analysis result reported in reference. Otherwise, it is assigned based on spectral classification.

<sup>3</sup> The Image Reduction and Analysis Facility (IRAF) is distributed by the Association of Universities for Research in Astronomy, Inc., under contract to the National Science Foundation.

TABLE 2  
OBSERVED STARS WITH COMPLETE SPECTRAL COVERAGE

HD	Other	Type	Observations	T <sub>e</sub>	L	M	[Fe/H]	E <sub>B-V</sub>	Ref	HD	Other	Type	Observations	T <sub>e</sub>	L	M	[Fe/H]	E <sub>B-V</sub>	Ref			
161817	s854402	A2V <sub>I</sub>	· E ·	J K	7636	3	-1	-1.13	0.06	FEH	191978	s49280	08.5III	· E ·	J K	35000	3	0	0.00	0.56 JHC		
106516	s157168	F5V	A · D ·	I ·	5929	4	-1	-0.57	0.00	FEH	16429	s12383	09.5III	· C · F ·	·	32000	3	0	0.00	0.91 JHC		
157089	s122301	F9V	· E ·	J K	5727	4	-1	-0.56	0.00	FEH	13494	s23043	B1III	· C · F ·	·	21500	3	0	0.00	0.47 JHC		
108177	s119389	G0V*	C D ·	I ·	6035	5	-1	-1.81	0.00	L	256413	s95626	B5III	· C · F ·	·	13800	3	0	0.00	0.56 JHC		
94028	s81555	G1V*	C D ·	I ·	5905	5	-1	-1.56	0.00	L	20023	s38671	B9III	· F G ·	·	11300	3	0	0.00	0.16 JHC		
148816	s121653	G1V*	· E ·	J K	5823	5	-1	-0.72	0.00	L	12027	s55163	A3III	· C · F ·	·	8300	3	0	0.00	0.16 JHC		
114762	s100458	G1V*	· D ·	H I ·	5818	5	-1	-0.79	0.00	L	240296	s35403	A6III	· F G ·	·	8000	3	0	0.00	0.34 JHC		
160693	s862228	G2V*	· E ·	J K	5718	5	-1	-0.50	0.00	L	12161	s12086	A8III	· C · F ·	·	7600	3	0	0.00	0.63 JHC		
117858	s63594	G2V*	· E ·	H I ·	5713	5	-1	-0.61	0.00	L	64191	s116066	F0III	· C · F ·	·	7030	3	0	0.00	0.03 JHC		
141335	s16836	G5V*	D ·	J K	5643	5	-1	-0.95	0.00	L	5211	s21831	F4III	· F G ·	·	6500	3	0	0.00	0.06 JHC		
···	s100656	G5V*	· E ·	H I ·	5641	5	-1	-0.89	0.00	L	56030	s96705	F6III	· C · F ·	·	6300	3	0	0.00	0.06 JHC		
198300	s32884	G7V*	· E ·	J K	5590	5	-1	-0.87	0.00	L	···	s20603	F7III	· F G ·	·	6200	3	0	0.00	0.09 JHC		
···	s45746	G7V*	· E ·	J K	5567	5	-1	-0.25	0.00	L	15866	s55660	G0III	· C · F ·	·	5900	3	0	0.00	0.06 JHC		
···	s46878	G7V*	· E ·	J K	5537	5	-1	-0.51	0.00	L	25894	s76462	G2III	· C · F ·	·	5770	3	0	0.00	0.03 JHC		
115349	s63437	G7V*	· E ·	H I ·	5505	5	-1	-0.49	0.00	L	2506	s21431	G4III	· F G ·	·	5700	3	0	0.00	0.16 JHC		
188510	s105417	G7V*	· E ·	J K	5455	5	-1	-1.75	0.00	L	18240	s162551	C0	· E ·	J K	5040	3	0	-0.10	0.00 FEH		
···	s18109	G8V*	· E ·	J K	5404	5	-1	-0.29	0.00	L	141714	s84019	G5III-IV	D ·	J K	5010	3	0	0.00	0.00 TTCB		
147750	s102117	G9V*	· E ·	J K	5305	5	-1	-0.28	0.00	L	26514	s76499	G6III	· C · F ·	·	4970	3	0	0.00	0.19 JHC		
121249	s100763	G9V*	· E ·	H I ·	5301	5	-1	-0.24	0.00	L	245389	s58259	G8III	· C · F ·	·	4870	3	0	0.00	0.16 JHC		
···	s240-67	K0V*	· E ·	J K	5159	5	-1	-0.43	0.00	L	100006	s99637	K0III	· S55155	G9III	· F G ·	·	4800	3	0	0.00	0.06 JHC
231510	s104872	K0V*	· E ·	J K	5103	5	-1	-0.40	0.00	L	100006	s99637	K0III	· C · E ·	I ·	4755	3	0	0.02	0.00 FEH		
···	s49312	K0V*	· E ·	J K	5049	5	-1	-0.27	0.00	L	···	s55164	K0III	· F G ·	·	4720	3	0	0.00	0.06 JHC		
···	g150-11	K0V*	· E ·	H · K	5009	5	-1	-0.33	0.00	L	139195	s101640	K0III	D ·	H I ·	4541	3	0	-0.11	0.00 FEH		
108	s10973	Q6F	C ·	F ·	4030	2	0	0.00	0.50	JHC	33506	s112496	K2III	· C · F ·	·	4460	3	0	0.00	0.06 JHC		
16691	s23550	O5F	· F ·	F ·	39000	2	0	0.00	0.81	JHC	112989	s63288	K1III	D ·	H I ·	4460	3	0	-0.07	0.00 FEH		
225160	s10952	O8I	C ·	F	34200	2	0	0.00	0.59	JHC	154733	s84835	K4III	E ·	J K	4200	3	0	0.00	0.00 FEH		
50064	s114524	B1Ia	C ·	F	21500	0	0	0.97	JHC	21110	s56436	K4III	F G ·	·	4010	3	0	0.00	0.12 JHC			
···	s20899	B3I	· F G ·	· F G ·	15500	2	0	0.00	0.66	JHC	236547	s21753	K7III	· F G ·	·	3750	3	0	0.00	0.22 JHC		
192832	s9374	B5Ia	· E ·	J K	13800	2	0	0.00	1.06	JHC	141477	s101752	M0.5IIIab	E ·	J K	3660	3	0	0.00	0.00 M83		
17145	s23607	B8Ia	C ·	F	11300	2	0	0.00	0.88	JHC	139153	s64790	M1.5IIIb	D ·	J K	3660	3	0	0.00	0.00 M83		
···	s11344	A0IB	· F G ·	· F G ·	9850	2	0	0.00	0.84	JHC	144542	s29777	M1III	E ·	J K	3660	3	0	0.00	0.00 M83		
332757	s877116	A3Ia	· E ·	J K	8300	2	0	0.00	0.34	JHC	···	s63549	M3III	E ·	H I ·	3300	3	0	0.00	0.00 JHC		
9167	s11801	A7I	· F G ·	· F G ·	7880	2	0	0.00	0.91	JHC	109896	s119508	M3+III	C · E ·	I ·	3300	3	0	0.00	0.00 M83		
842	s21214	A9I	C ·	F	7200	2	0	0.00	0.44	JHC	129712	s83488	M3-III	E ·	J K	3300	3	0	0.00	0.00 M83		
9880	s37370	F0IB	· F G ·	· F G ·	7030	0	0	0.00	0.25	JHC	167006	s66737	M3III	E ·	J K	3300	3	0	0.00	0.00 M83		
12842	s22943	F3I	C ·	F	6500	2	0	0.00	0.66	JHC	110964	s82478	M4III	CD ·	I ·	3100	3	0	0.00	0.06 JHC		
17971	s12518	F7I	· F G ·	· F G ·	6200	2	0	0.00	0.53	JHC	123657	s44901	M4.5III	E ·	H I ·	3100	3	0	0.00	0.00 M83		
25361	s24392	G0IA	C ·	F	5900	2	0	0.00	0.38	JHC	132813	s16558	M4.5III	E ·	J K	3100	3	0	0.00	0.00 M83		
236429	s21446	G1II	· F G ·	· F G ·	5850	2	0	0.00	0.41	JHC	151061	s141344	M5-III	E ·	J K	2960	3	0	0.00	0.00 TTCB		
9548	s37325	K1IB	· F G ·	· F G ·	4580	2	0	0.00	0.28	JHC	···	s62808	M5III	E ·	H I ·	2950	3	0	0.00	0.00 JHC		
1069	s11069	K2I	· F G ·	· F G ·	4460	2	0	0.00	0.28	JHC	142143	s45758	M6-7SIII	E ·	J K	2800	3	0	0.00	0.00 M83		
1400	s11095	K5I	· F G ·	· F G ·	3780	2	0	0.00	0.06	JHC	126661	s101025	F0M	E ·	H I ·	7754	4	0	0.00	0.00 FEH		
132933	s120798	M0.5IIb	E ·	J K	3660	2	0	0.00	0.41	JHC	83140	s6933	F3IV	F ·	H H ·	6500	4	0	0.00	0.12 JHC		
97778	s81736	M3IIb	A · E ·	I ·	3300	0	0	0.00	0.83	JHC	107213	s82244	F8V	C D ·	I ·	6300	4	0	0.11	0.09 FEH		
···	s11810	O7.5III	· F G ·	· F G ·	37000	3	0	0.00	0.69	JHC	136202	s120946	F8III-IV	D ·	H I ·	6072	4	0	-0.12	0.00 FEH		

TABLE 2—Continued

HD	Other	Type	Observations	T <sub>e</sub>	L	M	[Fe/H]	E <sub>B-V</sub>	Ref	HD	Other	Type	Observations	T <sub>e</sub>	L	M	[Fe/H]	E <sub>B-V</sub>	Ref
136064	s16660	F9IV	... E . . . H I . .	6000	4	0	-0.03	0.00	FEH	187238	s87735	K3IAB-IB	... E . . . J K	4500	2	1	0.20	1.00	FEH
143761	s65024	G2V	... E . . . J K . . .	5793	4	0	-0.17	0.00	FEH	196725	s106342	K3IB	... E . . . J K	4500	2	1	0.22	0.50	FEH
78277	s80653	G2IV	... C . . F . . . .	5770	4	0	0.00	0.09	JHC	112127	s82554	K2IIICN2	... C . E . . . H I . .	5544	3	1	0.30	0.00	FEH
70178	s80124	G5IV	... C . . F . . . .	5660	4	0	0.00	0.19	JHC	103238	s28142	K3III	... C D . . . .	4210	3	1	0.50	0.00	FFBG
104304	s157041	G8IV	... A . . E . . I . .	5478	4	0	0.18	0.00	FEH	132345	s158946	K3IIICN2	... D . . . H I . .	4210	3	1	0.50	0.00	FFBG
215835	s34810	O5.5V	... C . . F G . . . .	44500	5	0	0.00	0.72	JHC	181984	s9366	K3IIICN1	... E . . . J K	4210	3	1	0.50	0.00	FFBG
44811	s95633	O7.5V	... C . . F . . I . .	35000	5	0	0.00	0.44	JHC	187287	s18287	B9P	... E . . . J K	13622	4	1	1.70	0.03	FEH
236894	s22694	O8V	... C . . F G . . . .	30000	5	0	0.00	0.56	JHC	178065	s124282	B9III	... E . . . J K	12293	4	1	0.90	0.00	FEH
237007	s12463	B0V	... C . . F G . . . .	26500	5	0	0.00	0.69	JHC	144206	s45865	B9III	... D . . . J K	11455	4	1	0.25	0.03	FEH
37767	s58354	B3V	... C . . F . . . .	15500	5	0	0.00	0.38	JHC	175132	s47874	B9PSI	... E . . . J K	11455	4	1	1.40	0.06	FEH
240344	s20734	B4V	... C . . F G . . . .	14500	5	0	0.00	0.78	JHC	102870	s119076	F8V	... A . D . . . I . .	6072	4	1	0.24	0.00	FEH
30584	s39800	B6V	... C . . F . . . .	12900	5	0	0.00	0.44	JHC	... . . .	s9943	G5V*	... E . . . J K	5667	5	1	0.34	0.00	L
116608	s44595	A1V	... E . . . H I . . . .	9500	5	0	0.00	0.12	JHC	128127	s16424	G8V*	... D . . . H I . .	5436	5	1	0.18	0.00	L
124320	s63984	A2V	... E . . . H I . . . .	9120	5	0	0.00	0.16	JHC	145675	s45933	K0V	... E . . . J K	5250	5	1	0.27	0.00	FEH
190785	s69382	A2V	... E . . . J K . . . .	9120	5	0	0.00	0.03	JHC	158133	s85110	K0V*	... E . . . J K	5230	5	1	0.20	0.00	L
221741	s20709	A3V	... C . . F G . . . .	8720	5	0	0.00	0.12	JHC	... . . .	s84091	K0V*	... D . . . J K	5172	5	1	0.26	0.00	L
9547	s37324	A5V	... C . . F . . . .	8260	5	0	0.00	0.19	JHC	... . . .	s100482	K0V*	... E . . . H I . .	5029	5	1	0.19	0.00	L
21619	s38904	A6V	... C . . F . . . .	8000	5	0	0.00	0.12	JHC										
23863	s76231	A7V	... C . . F G . . . .	7880	5	0	0.00	0.06	JHC										
9972	s11895	A8V	... C . . F . . . .	7600	5	0	0.00	0.03	JHC										
23733	s76210	A9V	... C . . F G . . . .	7200	5	0	0.00	0.09	JHC										
10032	s37400	F0V	... C . . F G . . . .	7030	5	0	0.00	0.06	JHC										
281989	s57199	F6V	... C . . F G . . . .	6300	5	0	0.00	0.06	JHC										
107132	s82235	F7V	... C . E . . . I . . .	6200	5	0	0.00	0.00	JHC										
187691	s105338	F8V	... C . E . . . J K . . .	6146	5	0	0.12	0.00	FEH										
149890	s65426	F9V*	... C . E . . . J K	5955	5	0	-0.15	0.00	L										
17647	s38396	G1V	... C . F . . . .	5850	5	0	0.00	0.16	JHC										
66171	s6424	G2V	... C . E . . . I . . .	5770	5	0	0.00	0.06	JHC										
119550	s100676	G2V*	... C . E . . . H I . . .	5746	5	0	0.11	0.00	L										
22193	s38976	G6V	... C . F . . . .	5600	5	0	0.00	0.03	JHC										
27685	s93895	G7V	... C . F . . . .	5540	5	0	0.00	0.06	JHC										
115043	s28679	G1VA	... E . . . H I . . . .	5538	5	0	-0.10	0.00	FEH										
150633	s102327	G7V*	... E . . . J K . . . .	5472	5	0	-0.04	0.00	L										
... . . .	g165-49	G8V*	... E . . . H I . . . .	5440	5	0	-0.24	0.00	L										
114094	s24232	K0V	... C . F . . . .	5433	5	0	-0.21	0.00	L										
149661	s141269	K2V	... E . . . J K . . . .	5362	5	0	0.01	0.00	FEH										
151541	s17200	G9V*	... E . . . J K . . . .	5354	5	0	0.12	0.00	L										
5351	s11483	K4V	... C . F . . . .	5340	5	0	0.00	0.38	JHC										
283916	s76803	K5V	... C . F G . . . .	5240	5	0	0.00	0.03	JHC										
119850	s100695	M2-V	... E . . . H I . . . .	4400	5	0	0.00	0.56	JHC										
... . . .	s81292	M4.5VE	... E . . . H I . . . .	3400	5	0	0.00	0.00	M83										
...			... H I . . .	3200	5	0	0.00	0.02	JHC										

*Column (7).*— $M$ : assigned metallicity class. Metal classes are (1) metal-rich:  $[Fe/H] \geq 0.15$ ; (0) metal-normal:  $-0.20 \leq [Fe/H] \leq 0.15$ ; (-1) metal-poor:  $[Fe/H] \leq -0.20$ . See “[Fe/H]” description for source of original metallicity measurement.

*Column (8).*— $[Fe/H]$ : measured  $[Fe/H]$ . If references code is L, FEH, LB, or FFBG, metallicity is based on stellar atmosphere analysis reported in reference. Otherwise, star is assumed to be solar metallicity. Laird et al. (1988) (reference L) values are really  $[M/H]$ , which closely follows  $[Fe/H]$ . See that reference for further discussion.

*Column (9).*— $E_{B-V}$ : adopted interstellar reddening.  $R_V$  assumed to be 3.2. See discussion below.

*Column (10).*—Ref: Original source of stellar data. Codes are FEH Cayrel de Strobel et al. (1985); FFBG, Faber et al. (1985); JHC, Jacoby et al. (1984); L, Laird et al. (1988); LB, Luck & Bond (1985); M83, Keenan (1983); and TTCB, Turnshek et al. (1985).

### 3. LIBRARY CREATION

#### 3.1. Data Postprocessing

Since the SOKP and JHCLIB data have higher spectral resolution than the MDM data, the bluer data was further processed to match the MDM data spectral resolution. In each case, sub-spectra were extracted between 3510–4600 Å and then Gaussian smoothed to the MDM spectral resolution. Finally, they were rebinned to 5 Å pixel<sup>-1</sup>.

Intercomparison of the individual spectra segments revealed significant wavelength shifts for a number of spectra. Such shifts are attributed to linear dispersion calibration errors. To remove these shifts, a cross-correlation technique based on the algorithm described in Tonry & Davis (1979) was used to measure subpixel shifts. For each of the three spectral regions, template spectra determined to have pixel shifts of zero were selected. Appropriate pixel shifts for all other subspectra were then determined via cross-correlation against the appropriate template. Spectra were then registered with the IRAF routine IMSHIFT using a fifth-order polynomial interpolator (see IRAF documentation for details). Tests indicate that this process was accurate to  $\sim 0.20$  pixel = 1 Å. This process insures that all the final composite spectra are on the same linear dispersion coordinate system. Residual nonlinear dispersion problems (e.g., dispersion compression due to higher order terms) may still be present.

After registration, composite spectra were formed by multiplicatively scaling the individual subspectra until the means of the overlap areas were equal. Data in these overlap regions were then averaged. The resultant composite spectra were normalized to 100 at 5450 Å.

Next, the effects of interstellar reddening were removed. Appropriate  $E_{B-V}$  values were derived by direct comparison to the JHCLIB stars, originally dereddened using the Schild (1977) reddening law. However, the Cardelli, Clayton, & Mathis (1989) reddening law was used here since it is based on more modern data and is analytic in form. Note that different reddening laws result in significantly different continuum shapes. JHCLIB stars were rereddened with the Schild law and then dereddened with the Cardelli et al. law using the  $E_{B-V}$  values listed in Jacoby et al. (1984). An  $R_V$  value of 3.2 was assumed.

The newly acquired spectra were automatically dereddened in the following manner. First, the reddened spectrum was cross-correlated against all stars in JHCLIB to find the closest spectral match. This automatic classification scheme differs primarily from similar cross-correlation based schemes (e.g., Kurtz 1984; Adorf 1986) in that the Tonry & Davis (1979) “R” value is used to quantify the goodness of match instead of the height of the correlation function (see Tonry & Davis 1979; Latham 1985; Wyatt 1985 for more discussion of this point). Since the adopted cross-correlation technique uses only the line information (Tonry & Davis 1979), reddening does not affect this process. Once a template is found,  $A_V$  is iteratively increased until the residuals between the template and object spectra are minimized. The result was inspected and sometimes manually corrected. Derived  $E_{B-V}$  values for reobserved JHCLIB stars agree with the published values to about  $\pm 0.05$ . Adopted  $E_{B-V}$  values are listed in Table 2.

The effects of telluric atmospheric absorption were not corrected but removed. In principle, the magnitude of these effects can be derived using observations of hot stars taken at similar times and airmasses as the program objects. The telluric absorption features can then be divided out. Unfortunately, many of the program stars were observed through variable cirrus making the satisfactory removal of telluric absorption next to impossible. Rather than make imperfect corrections, the spectral regions most affected by telluric absorption have been set to zero. This process primarily affects the TiO bands found in late type stars near the telluric “a” and “b” bands at  $\approx 6800$  and 7500 Å, respectively, and the potentially important M star luminosity indicator line, Na I  $\lambda 8190$  (see Boroson & Thompson 1991 for a recent discussion). These features are partially or completely deleted in the current library.

Finally, stars with similar TZG parameters and similar overall spectral characteristics were averaged to form the individual library stellar spectra. In this way, systematic effects such as inconsistent TZG parameter determination and inconsistent photometric calibration were reduced. Individual flux points more than  $3\sigma$  different from the mean were rejected. These final spectra were then normalized to 100 at 5450 Å.

The final library is listed in Table 3 which tabulates the final assigned spectral type for each average spectrum and the stars used to form that spectrum. Identifications prefixed by “s” are SAO numbers. All other identifications are HD numbers. The spectra are displayed in Figures 1–6.

As a consistency test, the  $U - B$  and  $B - V$  colors for each composite spectrum listed in Table 3 were synthesized using the methodology described in Jacoby et al. (1984). These synthesized colors were then compared to previously determined  $UBV$  colors published in the literature via computed color residuals. These “catalog” data are the means of the colors of the individual stars listed in Table 3 used to form the composite library star. The color residuals are equal to the synthesized color minus the catalog value. The Jacoby et al. (1984) zero-points were adjusted to force the means of these residuals to zero. The synthesized and catalog colors as well as the computed residuals are listed in Table 4. Table 4 also lists the sources of the catalog data. The majority of the catalog data are either the final dereddened colors listed in Table 2 of Jacoby et al. (1984) (reference J) or the Table 4 of Laird et al. (1988)

TABLE 3  
COMPOSITE LIBRARY STARS: INPUT DATA

	Type	Base Spectra	Type		Base Spectra
			46	B8I	
1	O5V	215835	46	A03I	17145 s11344,s87716
2	O7B0V	44811,242935,237007	47	A79I	9167,942 s37370,12842
3	B34V	37767,240344	48	F03I	s37370,12842
4	B6V	30584	49	F7I	17971
5	A13V	116608,190785,124320,221741	50	G01I	25361,s21446
6	A57V	9547,21619,23863	51	K12I	s37325,1069
7	A8V	9972	52	K5I	1400
8	A9F0V	23733,10032	53	M0II	132933
9	F67V	s57199,107132	54	M3II	97778
10	F89V	187691,s65426	55	C0	182040
11	G12V	17647,66171,s100676	56	RG5V	s9943
12	G68V	22193,27685,s102327,g165-49,g60-66	57	RG8V	s16424
13	G9K0V	149661,s17200,33278,23524,s66004,s84725	58	RK0V	145675,s85110,g137-69,s100482
14	K4V	5351	59	RK9IV	182308,178065,175132,144206
15	K5V	s76803	60	RF8IV	102870
16	M2V	119850	61	RK2III	112127
17	M4V	s81292	62	RK3III	181984,132345,102328
18	A7IV	126661	63	RK3I	196725,187238
19	F3IV	83140	64	WG01V	108177,94028
20	F89IV	107213,136202,136064	65	WG12V	148816,114762,s66228,s63594
21	G2IV	143761,78277	66	WG5V	s16836,s100656
22	G5IV	70178	67	WG7V	s32884,s45746,s46678,s63437
23	G8IV	104304	68	WG8K0V	s18109,s102117,s100763,g240-67,s104872,s49312,g150-11
24	O7B1III	s11810,191978,16429,13494	69	WF5IV	106516
25	B5III	256413	70	WF9IV	157089
26	B9III	20023	71	WA2IV	161817
27	A3III	12027	72		
28	A6F0III	240296,12161,64191			
29	F47II	5211,56030,s20603			
30	G4III	15866,25894,2506			
31	G56III	141714,26514,s55155			
32	G8K0III	100006,245389,s55164,139195			
33	K2III	33506,112989			
34	K4III	154733,21110			
35	K7III	s21753			
36	M01III	141477,144542,139153			
37	M3III	167006,129712,109896,s63349			
38	M4III	110964,132813			
39	M5III	123657,s62808			
40	M6III	151061			
41	M7SII	142143			
42	O56II	10816691			
43	O8I	225160			
44	B1I	50064			
45	B35I	s20899,192832			

TABLE 4  
COMPOSITE LIBRARY STARS: SYNTHESIZED VERSUS CATALOG  $UBV'$  COLORS

Type	Synthesized		Catalog		Residuals		Type	Synthesized		Catalog		Residuals		References	
	U-V	B-V	U-V	B-V	U-V	B-V		U-V	B-V	U-V	B-V	U-V	B-V		
1	O5V	-1.10	-0.36	-1.08	-0.33	-0.02	-0.03	J	46	B8I	-0.63	-0.02	0.02	-0.02	J
2	O7B0V	-1.08	-0.31	-1.06	-0.30	-0.02	-0.01	J	47	A03I	-0.33	0.04	-0.40	0.08	J
3	B34V	-0.67	-0.20	-0.71	-0.17	0.04	-0.03	J	48	A79I	0.04	0.12	0.03	0.15	J
4	B6V	-0.38	-0.15	-0.42	-0.13	0.04	-0.02	J	49	F03I	-0.08	0.18	-0.11	0.20	J
5	A13V	0.03	0.08	-0.02	0.06	0.05	0.02	J	50	F7I	0.32	0.58	0.27	0.60	J
6	A57V	0.00	0.17	-0.04	0.12	0.04	0.05	J	51	G01I	0.71	0.85	0.65	0.89	J
7	A8V	0.22	0.28	0.18	0.34	0.04	-0.06	J	52	K12I	1.33	1.20	1.44	1.22	J
8	A9F0V	0.02	0.30	0.00	0.31	0.02	-0.01	J	53	K5I	1.77	1.52	1.87	1.56	J
9	F67V	0.01	0.49	0.01	0.50	0.00	-0.01	J	54	M0II	1.60	1.54	1.56	1.52	J
10	F89V	0.06	0.57	0.03	0.54	0.03	0.03	JS	55	M3II	1.81	1.66	1.85	1.66	J
11	G12V	0.12	0.60	0.18	0.62	-0.06	-0.02	JLS	56	C0	0.91	1.12	0.63	1.09	J
12	G68V	0.27	0.70	0.24	0.69	0.03	0.01	JLS	57	RG5V	0.73	0.81	0.68	0.68	ND/L
13	G9K0V	0.53	0.81	0.48	0.80	0.05	0.01	JLS	58	RG8V	0.49	0.78	0.33	0.73	SL
14	K4V	0.93	0.98	1.04	1.05	-0.11	-0.07	J	59	RK0V	0.70	0.88	0.56	0.85	JSL
15	K5V	1.29	1.24	1.34	1.24	-0.05	0.00	J	60	RB9IV	-0.38	-0.11	-0.38	-0.08	S
16	M2V	1.20	1.47	1.11	1.44	0.09	0.03	S	61	RF8IV	0.12	0.58	0.11	0.55	S
17	M4VE	1.15	1.54	1.08	1.55	0.07	-0.01	S	62	RK2II	1.55	1.29	1.42	1.26	S
18	A7IV	0.18	0.28	0.23	0.23	-0.05	0.05	S	63	RK3II	1.64	1.29	1.46	1.26	S
19	F3IV	0.00	0.37	0.01	0.40	-0.01	-0.03	J	64	RK3I	1.13	1.19	1.37	1.04	S
20	F89IV	0.09	0.55	0.07	0.53	0.02	0.02	J	65	WG01V	-0.17	0.44	-0.20	0.45	S
21	G2IV	0.20	0.62	0.21	0.48	-0.01	0.14	JS	66	WG12V	0.02	0.58	-0.04	0.57	SL
22	G5IV	0.40	0.71	0.43	0.72	-0.03	-0.01	J	67	WG5V	-0.01	0.60	-0.06	0.58	SL
23	G8IV	0.46	0.81	0.44	0.77	0.02	0.04	J	68	WG7V	0.13	0.65	0.65	0.63	ND/SL
24	O7B1III	-1.05	-0.31	-1.01	-0.27	-0.04	-0.04	J	69	WG8K0V	0.35	0.78	0.25	0.76	SL
25	B5III	-0.78	-0.18	-0.77	-0.14	-0.01	-0.04	J	70	WF5IV	-0.08	0.50	-0.13	0.46	S
26	B9III	-0.32	-0.11	-0.35	-0.08	0.03	-0.03	J	71	WF9IV	-0.03	0.59	-0.02	0.60	S
27	A3III	-0.02	0.06	-0.06	0.08	0.04	-0.02	J	72	WA2IV	-0.02	0.14	0.15	0.16	S
28	A6F0III	0.05	0.25	-0.02	0.25	0.07	0.00	J	73	W0I	0.01	0.01	0.01	0.01	ND
29	F47III	0.03	0.46	-0.01	0.47	0.04	-0.01	J	74	W1I	0.02	0.02	0.02	0.02	S
30	G04III	0.38	0.71	0.44	0.75	-0.06	-0.04	J	75	W2I	0.03	0.03	0.03	0.03	S
31	G56III	0.33	0.82	0.51	0.88	-0.18	-0.06	JS	76	W3I	0.04	0.04	0.04	0.04	S
32	G8K0III	0.83	1.01	0.82	1.00	0.01	0.01	J	77	W4I	0.05	0.05	0.05	0.05	S
33	K2III	1.16	1.15	1.18	1.17	-0.02	-0.02	J	78	W5I	0.06	0.06	0.06	0.06	S
34	K4III	1.63	1.38	1.67	1.37	-0.04	-0.04	J	79	W6I	0.07	0.07	0.07	0.07	S
35	K7III	1.91	1.49	2.00	1.55	-0.09	-0.09	J	80	W7I	0.08	0.08	0.08	0.08	S
36	M01III	1.98	1.62	1.96	1.60	0.02	0.02	J	81	W8I	0.09	0.09	0.09	0.09	S
37	M3III	1.90	1.62	1.92	1.61	-0.02	-0.02	J	82	W9I	0.10	0.10	0.10	0.10	S
38	M4III	1.61	1.49	1.67	1.58	-0.06	-0.06	J	83	W10I	0.11	0.11	0.11	0.11	S
39	M5III	1.10	1.47	1.26	1.52	-0.16	-0.05	J	84	W11I	0.12	0.12	0.12	0.12	S
40	M6III	1.71	1.72	1.64	1.79	0.07	-0.07	J	85	W12I	0.13	0.13	0.13	0.13	S
41	M7SIII	0.63	1.61	1.61	1.61	....	....	ND	86	W13I	0.14	0.14	0.14	0.14	S
42	O56IF	-1.11	-0.33	-1.08	-0.30	-0.03	-0.03	J	87	W14I	0.15	0.15	0.15	0.15	S
43	O8I	-1.08	-0.31	-1.07	-0.31	-0.01	-0.01	J	88	W15I	0.16	0.16	0.16	0.16	S
44	B1I	-0.98	-0.18	-1.00	-0.14	-0.02	-0.02	J	89	W16I	0.17	0.17	0.17	0.17	S
45	B35I	-0.73	-0.14	-0.76	-0.10	0.03	-0.04	J	90	W17I	0.18	0.18	0.18	0.18	S

(reference L). The remainder of the data was taken from a Simbad data base search (reference S) and comes from a variety of sources. The Simbad data was dereddened using the extinction values listed in Table 2 under the assumption that  $E(U - B) \approx 0.7 E(B - V)$ . A few stars in Tables 2 and 3 had no previously published color data (reference ND in Table 4). Multiple reference codes indicate that colors from multiple references were used to form the final catalog color. The final catalog value is the mean of all available color measurements if multiple measurements existed in the literature or multiple stars were used to form the final library star.

The standard deviations of the  $U - B$  and  $B - V$  residuals are 0.08 and 0.04 mag, respectively. Most of this scatter can be attributed to extinction correction uncertainties, estimated to be  $\sim 0.05$  mag. The larger  $U - B$  scatter may be in part due to the incomplete coverage of the U bandpass by the presented composite spectra. It is concluded that the synthesized colors are generally consistent with previously published  $UBV$  data confirming the accuracy of the stellar continuum of the composite library stars.

#### 4. INTERLIBRARY COMPARISON

Before the advent of digital technology, stellar libraries were based on photographic data and were used to make qualitative comparisons, such as spectral classification of stars on photographic objective prism plates (e.g., Houk & Newberry 1984).

The quantitative accuracy of these libraries was not critical. Although modern, digital stellar libraries can be also be used qualitatively, it is more common to put them to quantitative use in direct comparison with other data sets. Such quantitative comparisons, however, require a certain level of internal consistency between the data sets being compared. In theory, accurate spectrophotometry should allow accurate comparisons. In practice, not all currently available digital stellar libraries appear to be of equal spectrophotometric quality. Moreover, all published libraries have different spectral resolutions and wavelength baselines making some manipulation necessary before direct comparisons can be made. Thus, all digital stellar libraries must be used cautiously in any quantitative application. These points can be illustrated by comparing JHCLIB to PICKLIB and to the new library presented here.

To compare JHCLIB and PICKLIB, several steps are necessary. Since JHCLIB spectra represent individual stars and PICKLIB spectra are formed from the combination of individual stellar spectra, appropriate JHCLIB stars must be selected and averaged together first. These composite JHCLIB spectra were then Gaussian smoothed and rebinned to the PICKLIB spectral resolution and sampling, respectively. Finally, all processed spectra were renormalized to 100 at 5450 Å.

Comparison of these processed JHCLIB stars to their PICKLIB analogs provides examples of both good and poor spectral agreement. Examples of good agreement are shown in Figure 7. In Figures 7a and 7b, the PICKLIB K01V spectrum is com-

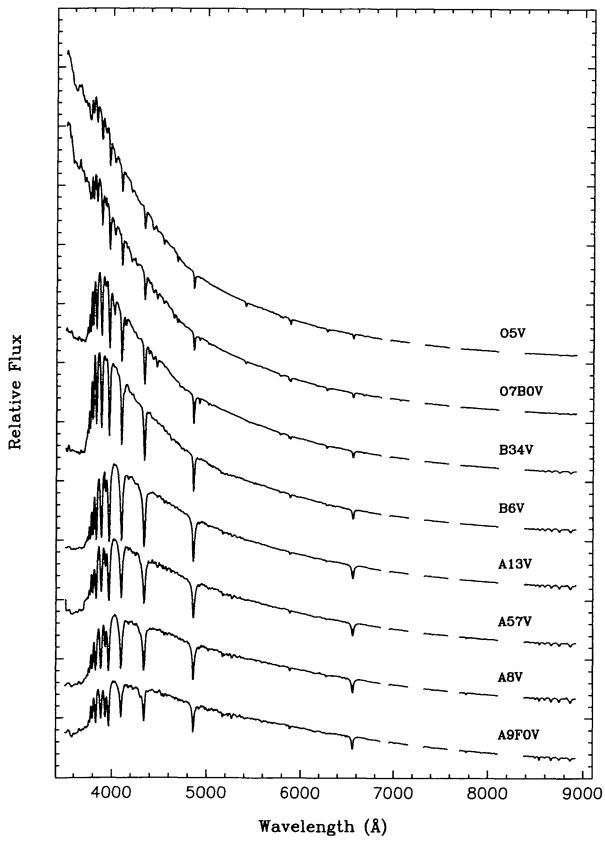
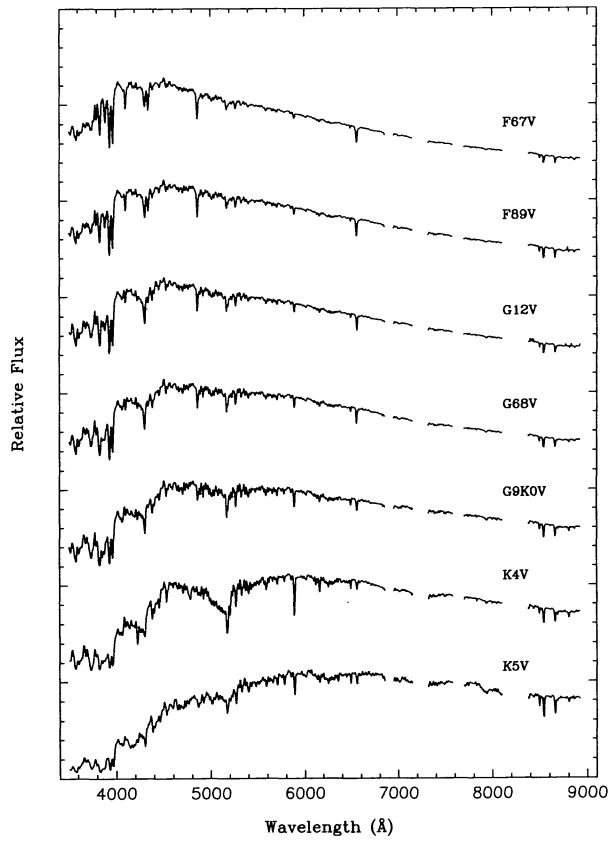


FIG. 1.—Dwarf-type library stars. Near-IR gaps are excised telluric absorption bands. All spectra have been normalized to 100 at 5450 Å. Major tick marks on “Relative Flux” axis are separated by 100 relative units. The M dwarf library stars are displayed with the M giants in Fig. 3.



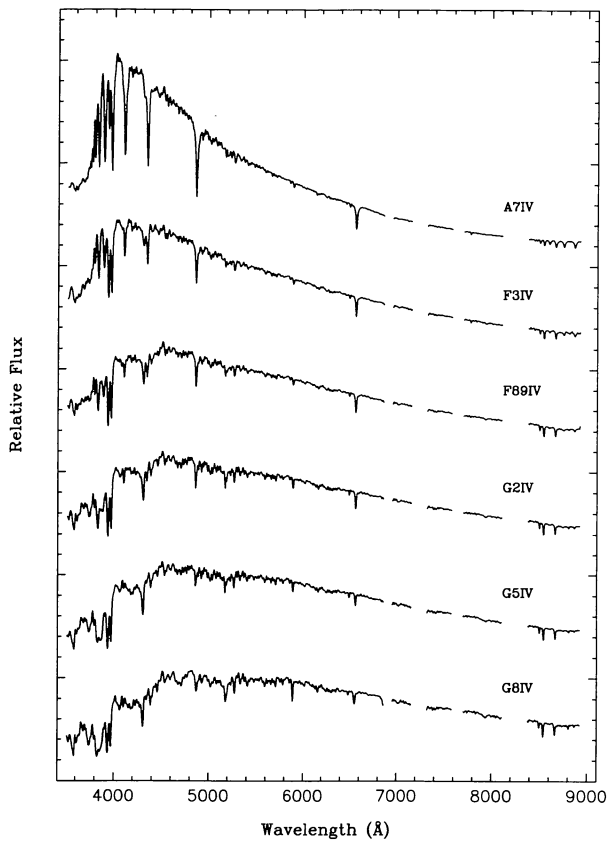


FIG. 2.—Subgiant-type library stars. Near-IR gaps are excised telluric absorption bands. All spectra have been normalized to 100 at 5450 Å. Major tick marks on “Relative Flux” axis are separated by 100 relative units.

pared to a K01V spectrum formed from JHCLIB stars 51 and 52, HD 29050 and HD 23524, respectively. In Figures 7c and 7d, the PICKLIB G58III spectrum is compared to a G58III spectrum formed from JHCLIB stars 90, 92, and 94, BD + 28°1885, HD 26514, and HD 249240, respectively. The residual spectra are defined as

$$R_i = 1.0 - \frac{\text{JHCLIB}_i}{\text{PICKLIB}_i}. \quad (1)$$

High-frequency differences are certainly due to a combination of inexact spectral resolution matches, spectral misalignments, and intrinsic physical differences between the stars actually observed. The continua agree reasonably well.

On the other hand, the continua of many blue PICKLIB stars diverge significantly from analogous JHCLIB combinations below 4000 Å. Examples are provided in Figure 8. In Figures 8a and 8b, the PICKLIB B13V spectrum is compared to a composite formed from JHCLIB stars 11, 12, 13, and 14, HD 158695, HD 237007, HD 35215, and HD 37767, respectively. The JHCLIB composite formed from stars 19 and 20, HD 116608 and Feige 41, respectively, is compared to the PICKLIB B69V star in Figures 8c and 8d. In these bluer stars, the continua are clearly inconsistent below 4000 Å.

The new data presented here and the JHCLIB stars appear to be more consistent. Ten of the individual JHCLIB stars have been completely reobserved. These newly acquired spectra can be directly compared to published JHCLIB spectra of the same star. To make this comparison, the JHCLIB stars must again be smoothed, rebinned, and normalized as described above. Individual JHCLIB spectra were compared to individual stellar spectra, as listed in Table 2, not the final composite spectra listed in Table 3. From the 10 comparisons possible, the two best and the two worst are shown in Figures 9 and 10, respectively. In these figures, the residuals are defined as

$$R_i = 1.0 - \frac{\text{JHCLIB}_i}{\text{NewData}_i}. \quad (2)$$

The actual stars compared are indicated on the figures. The overall agreement in Figure 9 is quite good with continua differences likely due to a combination of spectrophotometric calibration and dereddening differences. The continua differences in Figure 10 are more pronounced but likely due to the same causes. There is no way of assessing which dataset is absolutely “less” accurate in this regard. In Figures 9 and 10, spectral misalignment is more apparent than in Figure 7 and 8. This suggests that the new spectra, although internally consistent, may be slightly misregistered relative to the global coordinate system.

In short, these comparisons demonstrate the kind of quantitative differences that can exist between individual spectrophotometric data sets. Thus caution must be exercised when intercomparing and/or intermixing different data sets. Specifically, there appear to be serious inaccuracies in the blue PICKLIB stars below 4000 Å. This makes the use of PICKLIB inappropriate for certain classes of problems (e.g., spectral synthesis of young, composite populations).

## 5. CONCLUSION

This new library offers several advantages over previously published stellar libraries. It is photometrically well-calibrated individually and consistently from star to star. Good temperature and luminosity coverage has been achieved. An astrophysically useful wavelength baseline has been spanned. Finally, the incorporation of stars with well-determined TZG parameters increases the accuracy of the spectral type assigned to each composite library star.

The next step is clear. A higher spectral resolution library which extends both into the vacuum UV and the near-IR K-band is now technologically possible. The most pressing astrophysical need to is incorporate as many metal-rich stars as possible. Ideally, three grids should be constructed with [Fe/H] ≈ -1.0, 0.0, and 0.6. Realistically, the construction of a complete metal-rich grid seems infeasible in the near future despite recent progress being made on giants in Baade’s window (Rich 1988). Complete metal-rich coverage may have to rely on the new, more accurate stellar atmospheres models now becoming available (Kurucz 1991). Nevertheless, work should continue on improving current empirical metal-poor and solar metallicity grids as promptly as possible.

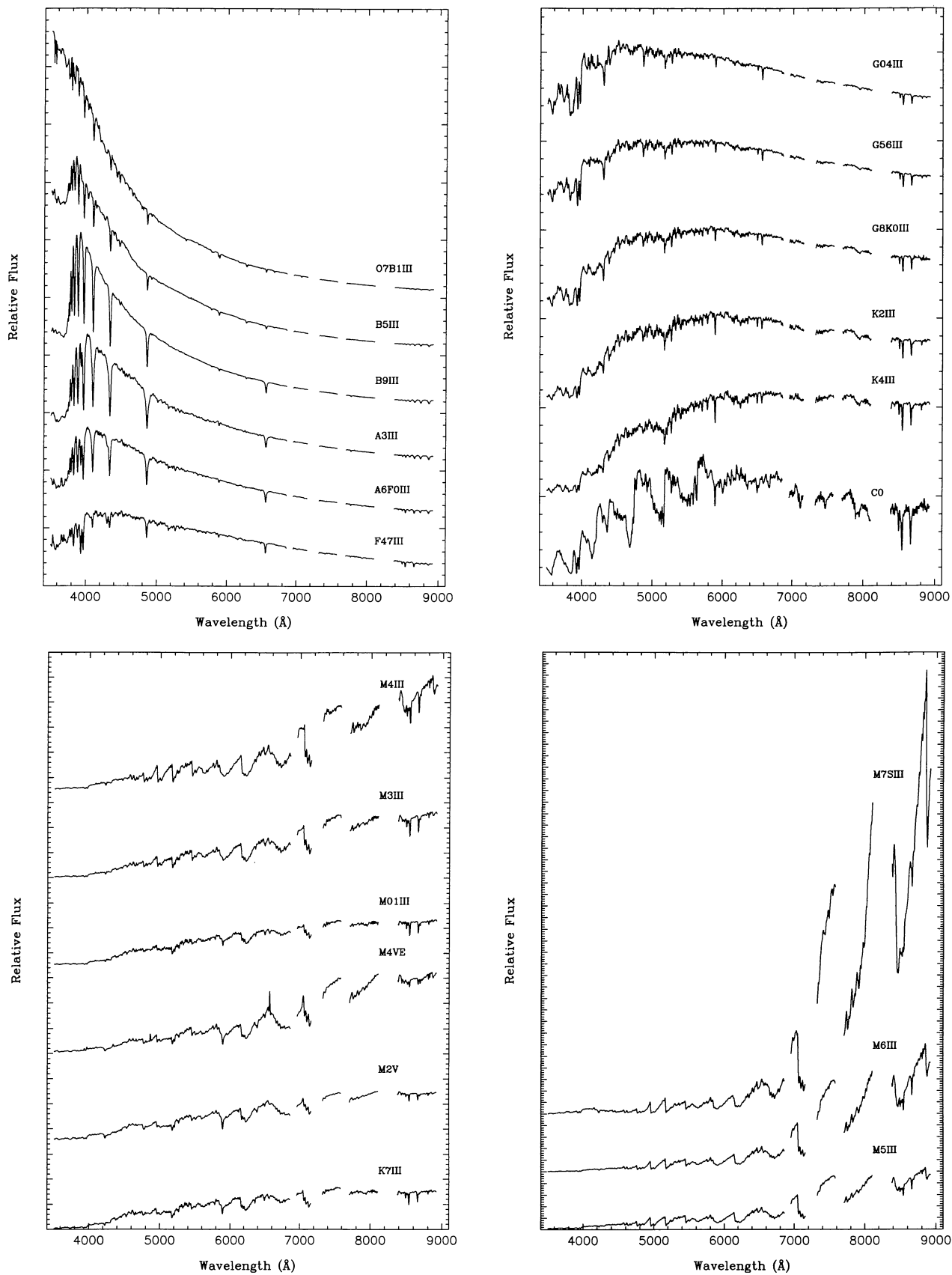


FIG. 3.—Giant-type library stars. Near-IR gaps are excised telluric absorption bands. All spectra have been normalized to 100 at 5450 Å. Major tick marks on “Relative Flux” axis are separated by 100 relative units.

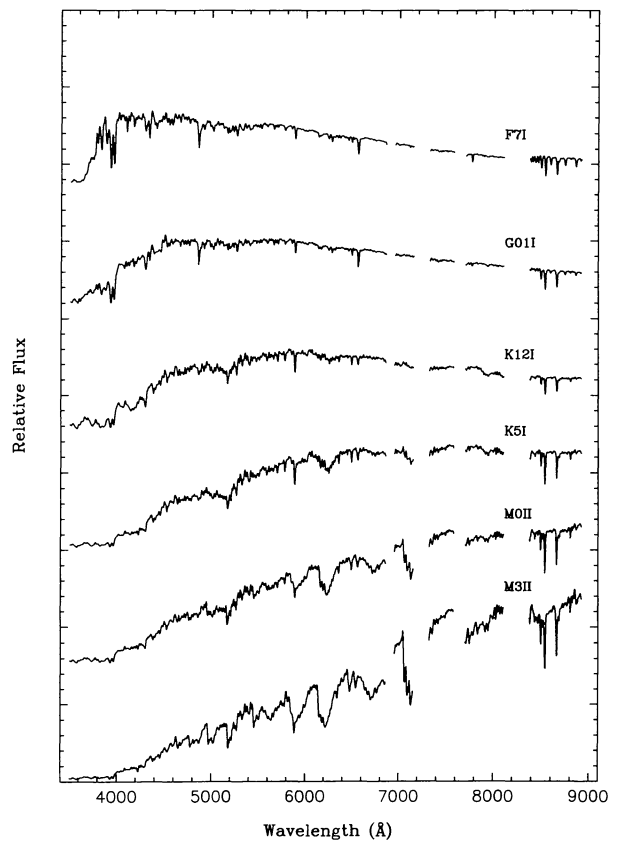
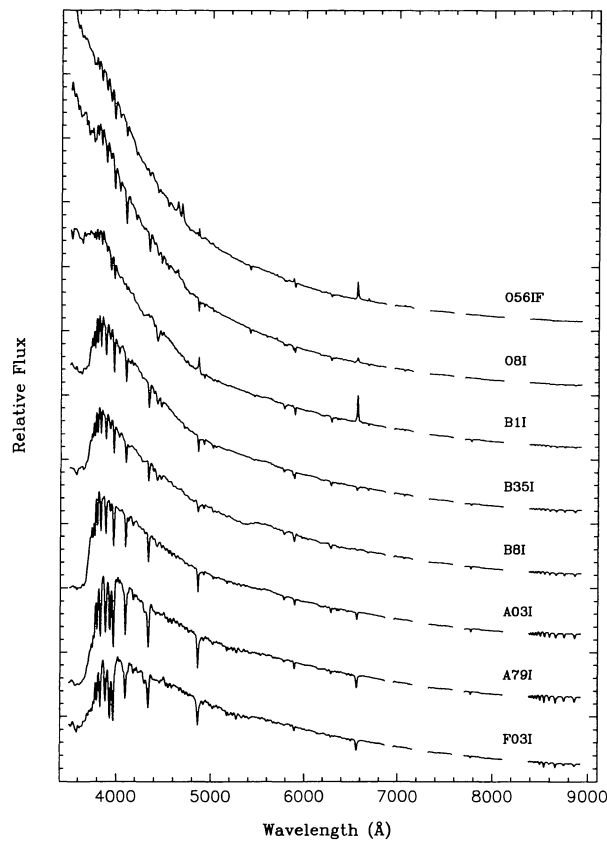


FIG. 4.—Supergiant-type library stars. Near-IR gaps are excised telluric absorption bands. All spectra have been normalized to 100 at 5450 Å. Major tick marks on “Relative Flux” axis are separated by 100 relative units.

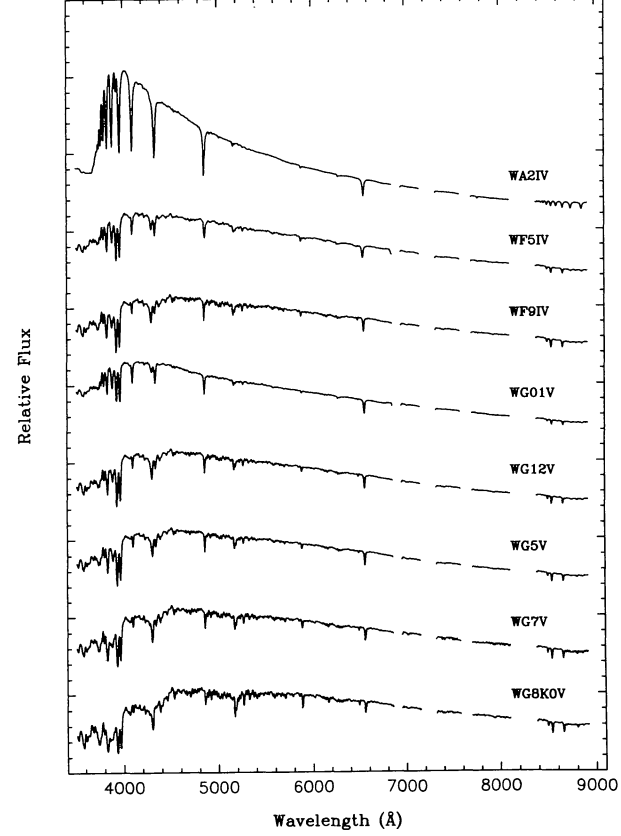
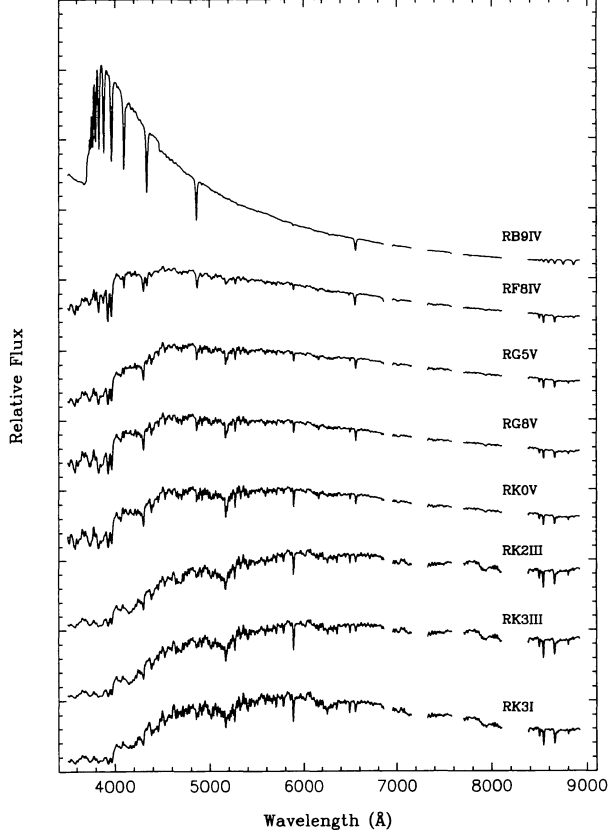


FIG. 5.—Metal-rich library stars. Near-IR gaps are excised telluric absorption bands. All spectra have been normalized to 100 at 5450 Å. Major tick marks on “Relative Flux” axis are separated by 100 relative units.

FIG. 6.—Metal-poor library stars. Near-IR gaps are excised telluric absorption bands. All spectra have been normalized to 100 at 5450 Å. Major tick marks on “Relative Flux” axis are separated by 100 relative units.

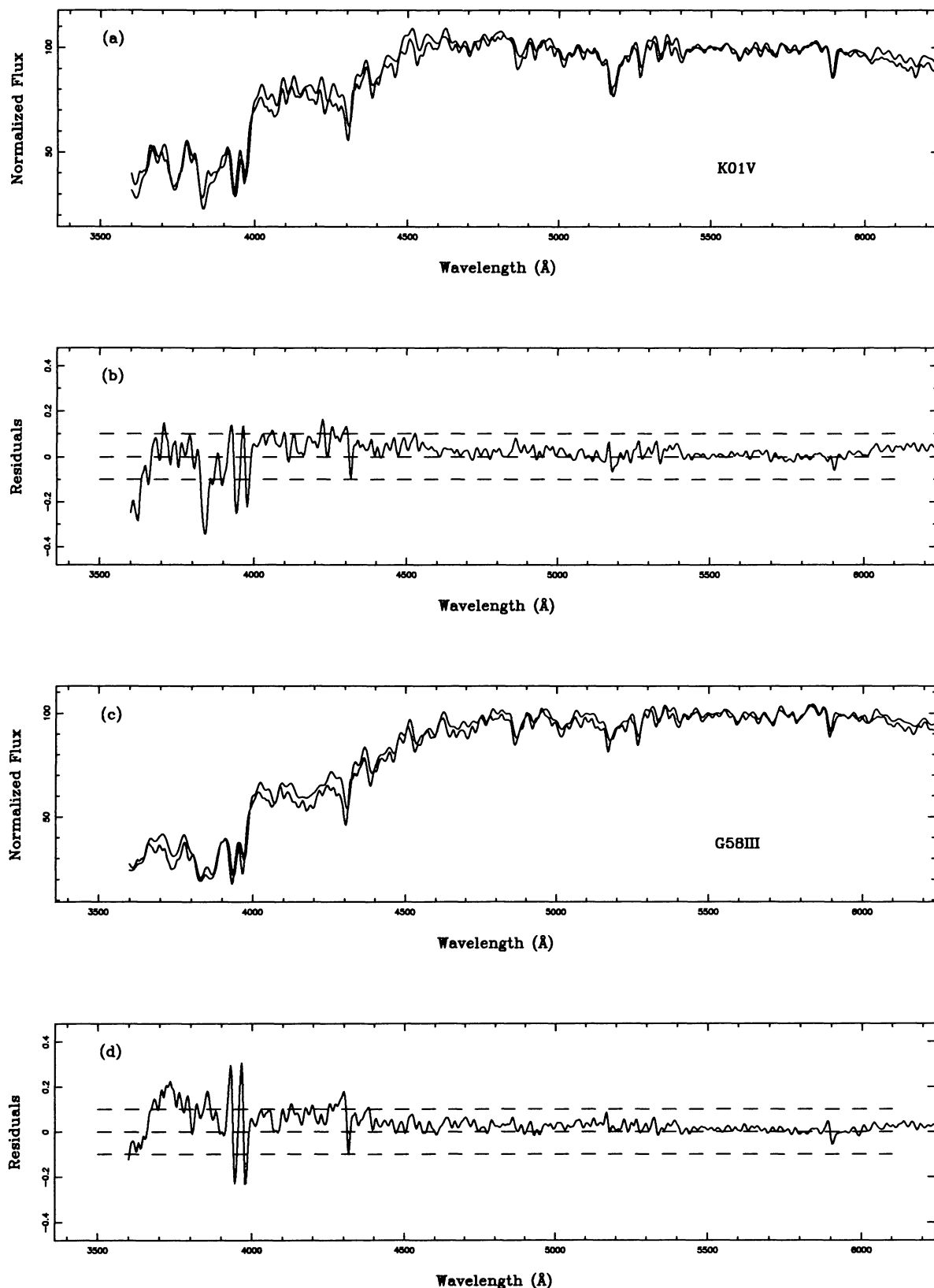


FIG. 7.—Comparison of JHCLIB and PICKLIB: Well-matched stars. Negative residuals indicate that the composite JHCLIB spectrum has more relative flux at that point than the comparison PICKLIB spectrum.

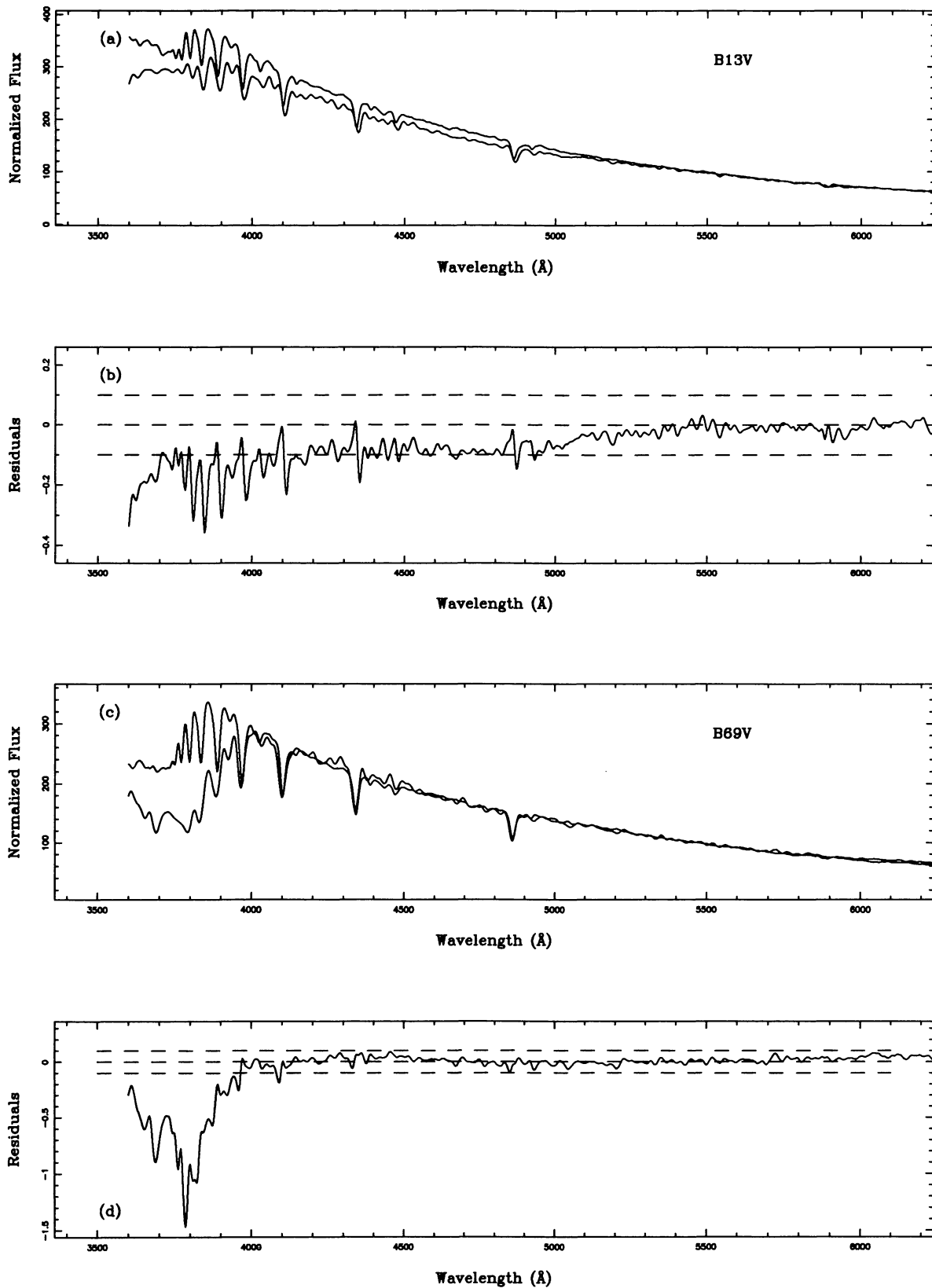


FIG. 8.—Comparison of JHCLIB and PICKLIB: poorly matched stars. Negative residuals indicate that the composite JHCLIB spectrum has more relative flux at that point than the comparison PICKLIB spectrum. In this figure, the PICKLIB spectra lie almost exclusively below the composite JHCLIB spectra.

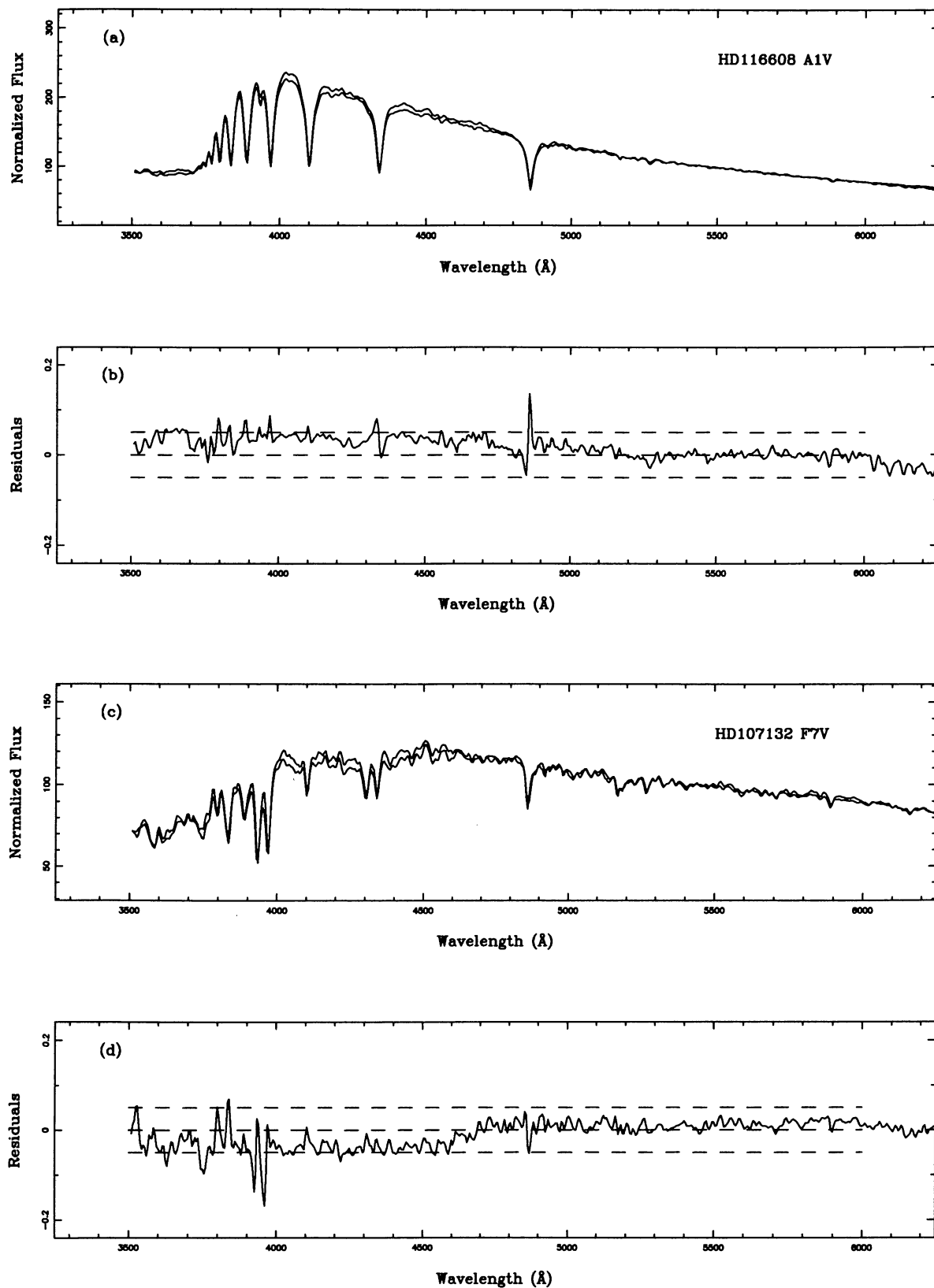


FIG. 9.—Comparison of JHCLIB and New Data: Well-matched stars. Negative residuals indicate that the JHCLIB spectrum has more relative flux at that point than the newly observed spectrum of the same star.

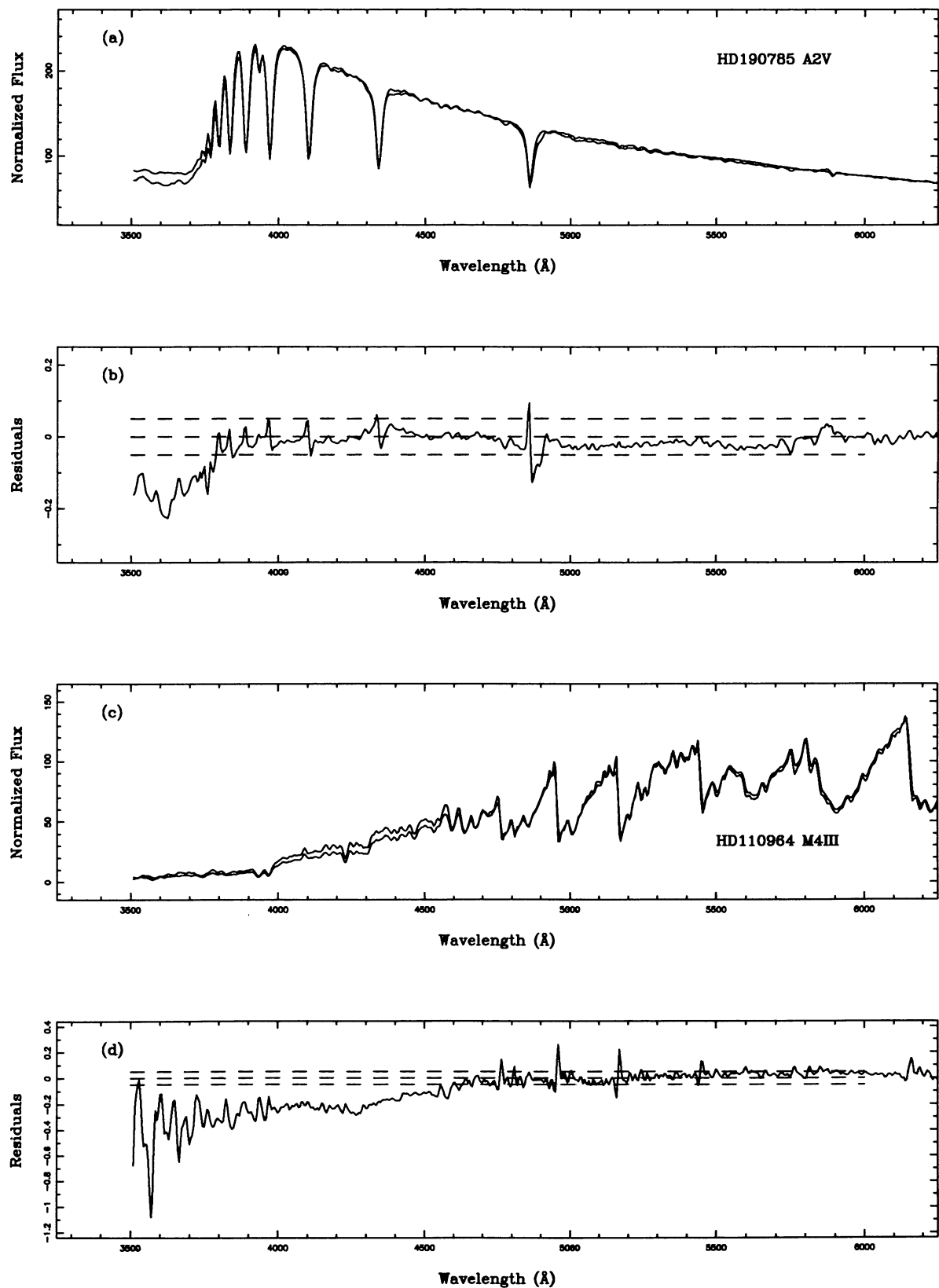


FIG. 10.—Comparison of JHCLIB and New Data: Poorly matched stars. Negative residuals indicate that the JHCLIB spectrum has more relative flux at that point than the newly observed spectrum of the same star.

This work is based in part on a thesis submitted by D. R. S. in partial fulfillment of the requirements for a degree of Doctor of Philosophy in Astronomy in the Horace H. Rackham School of Graduate Studies at the University of Michigan. D. R. S. acknowledges generous financial support while a graduate student at the University of Michigan from the Department of Astronomy, the Rackham School of Graduate Studies, the Ralph W. Baldwin Fellowship fund, and the Clinton B. Ford Fellowship fund. The authors thank the University of Arizona and University of Michigan TAC's for the generous allocations of time necessary for completion of this project. Bob Barr, Larry Breuer, and especially Matt Johns helped

make our runs at the Hiltner 2.4 m particularly enjoyable and productive. We thank Mike Dinniman and Rex Saffer for assistance in obtaining some of the SOKP data. Some data for this paper were obtained from the Astronomical Data Center at the NASA Goddard Space Flight Center and from the Simbad data base operated at CDS, Strasbourg, France. We thank John Laird for providing his stellar data base ahead of publication and Greg Bothun for commentary on earlier versions of this paper. We also thank the anonymous referee for a careful reading of the paper and suggesting the use of synthesized colors. As always, we thank Paula Christianson-Silva for funding and patience during all our joint endeavors.

## APPENDIX A COMPUTER-READABLE VERSION OF THE LIBRARY

A computer-readable version of the library described here has been prepared. It has been submitted to the Astronomical Data Center at the NASA Goddard Space Flight Center and is also available from D. R. S. via anonymous ftp upon request (see the AAS Directory for the most recent E-mail addresses of authors).

The submitted file consists of the dereddened, telluric absorption line excised spectra listed in Table 3 and shown in Figures 1–6. Each spectrum consists of 110 free format lines of data. The field separators are ASCII SPACE characters, and each line is terminated by an ASCII NEWLINE character. The first line contains the number of the star and the spectral type as tabulated in Table 3. The next 109 lines consist of 10 FORTRAN F7.3 normalized flux points, except for the last line which only lists 4 values. Each spectrum has a total of 1084 values. The first pixel has a central wavelength of 3510 Å. The dispersion is 5 Å pixel<sup>-1</sup>. Each spectrum has been normalized to 100 at 5450 Å. It is emphasized that these spectra are the end product of the processing scheme described above. The individual calibrated and un-dereddened spectra cannot be recovered from the distributed spectra (see Jacoby et al. [1984] for an alternative). There are a total of 72 spectra and hence 7920 lines of information.

## REFERENCES

- Adorf, H.-M. 1986, in *Data Analysis in Astronomy II*, ed. V. Di Gesù, L. Scasi, P. Craine, J. H. Friedman, & S. Levialdi (New York: Plenum), 61
- Barnes, J. V., & Hayes, D. S. 1982, IRS Standard Star Manual (Kitt Peak Obs. Pub.)
- Breger, M. 1976, ApJS, 32, 1
- Boroson, T. A., & Thompson, I. 1991, AJ, 101, 111
- Cardelli, J. A., Clayton, G. C., & Mathis, J. S. 1989, ApJ, 345, 245
- Cayrel de Strobel, G., Bentolila, C., Hauck, B., & Duquennoy, A. 1985, A&AS, 59, 145
- Faber, S. M., Friel, E. D., Burstein, D., & Gaskell, C. M. 1985, ApJS, 57, 711
- Filippenko, A. V. 1982, PASP, 94, 715
- Giclas, H. L., Burnham, R., & Thomas, N. G. 1972, The Lowell Proper Motion Survey: The Northern Hemisphere (Flagstaff: Lowell Obs.)
- . 1978, Lowell Obs. Bull., 164, 1
- Guiderdoni, B., & Rocca-Volmerange, B. 1987, A&A, 186, 1
- Gunn, J. E., & Stryker, L. L. 1983, ApJS, 52, 121
- Houk, N., & Newberry, M. V. 1984, A Second Atlas of Objective Prism Spectra (Ann Arbor: Dept. of Astronomy, University of Michigan)
- Jacoby, G. H., Hunter, D. A., & Christian, C. A. 1984, ApJS, 56, 257 (JNCLIB)
- Joly, M. 1974, A&A, 33, 177
- Keenan, P. C. 1983, Bull. Inf. Centre de Donnes Astronomiques de Strasbourg, 24, 1
- Kurtz, M. J. 1984, in *The MK Process and Stellar Classification*, ed. R. F. Garrison (Toronto: David Dunlap Obs.), 136
- Kurucz, R. L. 1991 in *Precision Photometry: Astrophysics of the Galaxy*, ed. AG Davis Philip, A. R. Upgren, & K. A. Janes (Schenectady: L. Davis), 27.
- Laird, J. B., Carney, B. W., & Latham, D. W. 1988, AJ, 95, 1843
- Latham, D. W. 1985, in *IAU Colloq. 88, Stellar Radial Velocities*, eds. A. G. D. Davis and D. W. Latham (Schenectady: Davis), 21
- Luck, R. E., & Bond, H. E. 1985, ApJ, 292, 559
- Luppino, G. A. 1989, PASP, 101, 931
- MacFarlane, M. J. 1979, Ph.D. thesis, Univ. of Texas
- Massey, P., & Gronwall, C. 1990, ApJ, 358, 344
- Massey, P., Strobel, K., Barnes, J. V., & Anderson, E. 1988, ApJ, 328, 315
- O'Connell, R. W. 1973, AJ, 78, 1074
- Pickles, A. J. 1985, ApJS, 59, 33 (PICKLIB)
- Pritchett, C., & van den Bergh, S. 1977, ApJS, 34, 101
- Rich, R. M. 1988, AJ, 95, 828
- Schild, R. E. 1977, AJ, 82, 337
- Schmidt-Kaler, Th. 1982, in *Landolt-Börnstein; Stars and Star Clusters; Numerical Data and Functional Relationships in Science and Technology, Group IV, Vol 2b*, ed. K. Schaifers & H. H. Voigt (Berlin: Springer), 1
- Silva, D. R. 1991, Ph.D. thesis, University of Michigan
- Spinrad, H., & Taylor, B. J. 1971, ApJS, 22, 445
- Strom, K. M. 1979, IIDS Standard Star Manual (Kitt Peak Obs. Pub.)
- Tony, J., & Davis, M. 1979, AJ, 84, 1511
- Turnshek, D. E., Turnshek, D. A., Craine, E., & Boeshaar, P. C. 1985, An Atlas of Digital Spectra of Cool Stars (Tucson: Western Research Co.)
- Wyatt, W. F. 1985, in *IAU Colloq. 88, Stellar Radial Velocities*, ed. A. G. D. Davis & D. W. Latham (Schenectady: Davis), 123